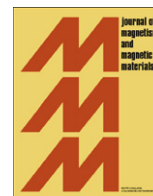




ELSEVIER

Contents lists available at SciVerse ScienceDirect

## Journal of Magnetism and Magnetic Materials

journal homepage: [www.elsevier.com/locate/jmmm](http://www.elsevier.com/locate/jmmm)

## Spin crossovers in Mott–Hubbard insulators at high pressures

I.S. Lyubutin<sup>a,\*</sup>, S.G. Ovchinnikov<sup>b</sup><sup>a</sup> Shubnikov Institute of Crystallography, RAS, 119333, Moscow, Russia<sup>b</sup> Kirensky Institute of Physics, Siberian Division of RAS, 660036, Krasnoyarsk, Russia

## ARTICLE INFO

Available online 25 February 2012

## Keywords:

Electronic structure  
Spin crossover  
High pressure  
Magnetic transition

## ABSTRACT

The high-pressure induced phase transitions initiated by electronic transition in 3d ions from the high-spin (HS) to the low-spin (LS) state (HS–LS spin-crossover) are considered. Behavior of the system with  $d^6$  electronic configuration is investigated in the ground state of zero temperature and critical pressure  $P_c$ . Magnetic properties of the Mott–Hubbard insulator  $(Mg_{1-x}Fe_x)O$  are studied in the vicinity of the quantum critical point  $(T=0, P_c)$ . At the critical pressure of spin crossover  $P_c$ , the spin gap energy  $\epsilon_S$  between HS and LS states is zero. The quantum spins fluctuations  $HS \Leftrightarrow LS$  do not require any energy, and the antiferromagnetism is destroyed in the quantum critical point by the first order transition.

© 2012 Published by Elsevier B.V.

## 1. Introduction

The transition-metal oxides are a very broad class of compounds with diverse physical properties that are important in both fundamental science and practical applications. This class includes high-temperature superconductors and materials with the giant magnetoresistance, multiferroics, materials for spintronics and optoelectronics, various magnetic and magneto-optical crystals. The mixed iron oxides and perovskite-like compounds are extremely important in geophysics.

The properties and the behavior of the transition-metal oxides are mainly governed by strong electron correlations, which are also responsible for the dielectric state of these materials [1]. One of important properties is the insulator–metal transitions (IMT), which can be caused, for example, by a change in the concentration of charge carriers (doping) or by the application of an internal (due to ion substitution) or external pressure. These phenomena are governed by a complex interaction of different parameters, including the width of the 3d-band  $W$ , the charge transfer energy  $D$  (the  $p$ – $d$  gap), and Coulomb repulsion  $U$  (the  $d$ SYMBOL 45 \f "Courier New" \s 12- $d$  or Mott–Hubbard gap). Depending on the relative values of these parameters, the system can be either a metal or an insulator. The majority of these systems has a partially filled 3d band and manifests antiferromagnetic ordering in the ground state.

An applied external pressure allows controlling correlation effects by changing the  $W$ ,  $U$ , or  $D$  parameters in a specific manner. This enables easily controlling the magnetic, structural, electronic, optical, and transport properties of solids. In such materials theory

predicts the pressure induced insulator–metal transition accompanied by the collapse of the localized magnetic moment and by a structural phase transition, but the expected critical pressures of such transformations are very high [2]. However, with the development of the high-pressure diamond-anvil-cell technique the experimental investigations of such transitions are now possible especially due to the synchrotron radiation facilities.

Recently, several synchrotron radiation and resonance techniques have been applied to perform the high-pressure experiments and to investigate the magnetic and crystal structures, electronic and transport properties of 3d metal oxides having different crystal structures [3]. The cubic monoxides  $(Mg,Fe)O$ ,  $NiO$  and yttrium iron garnet  $Y_3Fe_5O_{12}$ , the perovskite-like rare-earth orthoferrites  $RFeO_3$  ( $R=Nd, Lu, Y$ ) and multiferroic  $BiFeO_3$  crystals, the hematite  $Fe_2O_3$  with corundum structure, the rhombohedral iron borates  $FeBO_3$  and trigonal rare-earth borate  $GdFe_3(BO_3)_4$  were studied under high pressures up to 200 GPa created in diamond anvil cells at temperatures between 3.5 K and 2000 K [3]. The transmission Mössbauer (TMS) and synchrotron Mössbauer (SMS) spectroscopy, X-ray diffraction and the synchrotron high-resolution  $K\beta$  X-ray emission spectroscopy (XES), optical absorption spectroscopy, Raman scattering, electron microscopy, and the direct electro-resistivity measurements have been carried out.

2. Spin crossovers in  $d^5$  electronic configuration and phase transitions at high pressures

The evidence of the high-spin (HS) to low-spin (LS) transition (HS–LS spin-crossover) in a set of 3d metal oxides follows from the Mössbauer TMS and SMS measurements and it is supported by XES experiments [3,4]. An example of the Mössbauer TMS and

\* Corresponding author.

E-mail address: [lyubutin@magnet.crystal.msk.su](mailto:lyubutin@magnet.crystal.msk.su) (I.S. Lyubutin).

SMS data for iron borate  $\text{FeBO}_3$  is shown in Fig. 1 [5], whereas the Mössbauer SMS and X-ray emission XES data of Fig. 2 demonstrate the spin crossover effect in bismuth ferrite  $\text{BiFeO}_3$  [6,7]. The collapse of the iron magnetic moment in the crystals at pressures of about 40–55 GPa and radical drop of the local spin of

$3d^5$  ions are substantial evidences for the spin-crossover transition in such systems.

The HS-LS spin crossover in  $3d^5$  ( $\text{Fe}^{3+}$ ) ions is a transition

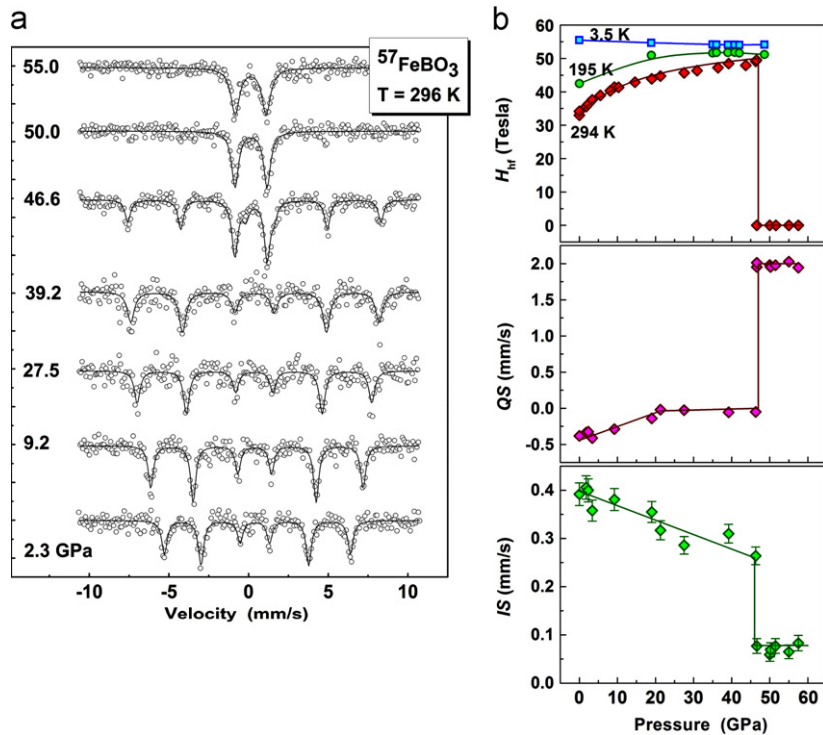
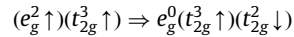


**Fig. 1.** Representative  $^{57}\text{Fe}$ -Mössbauer spectra (a) and pressure dependence of the Mössbauer hyperfine parameters (b) in the iron borate  $\text{FeBO}_3$  single crystal. Mössbauer parameters—the magnetic hyperfine field at iron nuclei  $H_{\text{hf}}$ , the quadrupole shift  $QS$ , and the isomer chemical shift  $IS$  indicate the spin transition in  $\text{Fe}^{3+}$  ions from the high-spin  $S=5/2$  ( ${}^6A_{1g}$ ) state to the low-spin  $S=1/2$  ( ${}^2T_{2g}$ ) state at pressure near 47 GPa. The spin transition is followed by magnetic collapse [5].

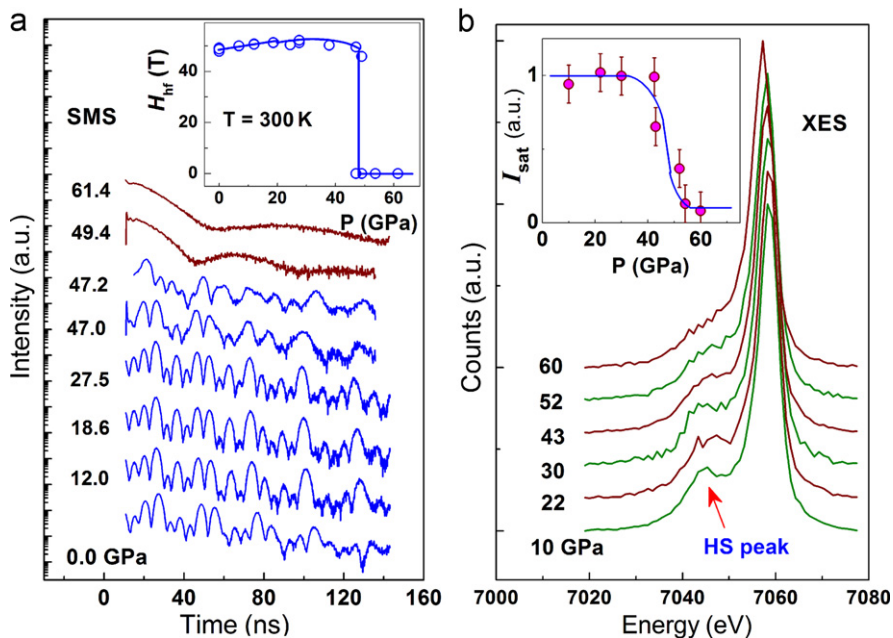


**Fig. 2.** High-pressure synchrotron Mössbauer SMS spectra (a) and the X-ray emission XES  $\text{Fe-K}_{\beta}$  spectra (b) in multiferroic  $\text{BiFeO}_3$ . Inset in (a) shows the disappearance of the magnetic hyperfine field ( $H_{\text{hf}}$ ) at Fe ions at pressure near 49 GPa demonstrating the collapse of the iron magnetic moment due to the spin HS-LS crossover. Inset in (b) indicates the pressure dependence of the relative intensity of the satellite HS-peak ( $I_{\text{sat}}$ ) in the  $\text{Fe-K}_{\beta}$  X-ray emission spectrum. At pressures  $P \approx 43$ –60 GPa the satellite intensity decreases showing the spin transition from  $S=5/2$  to  $S=1/2$  [6,7].

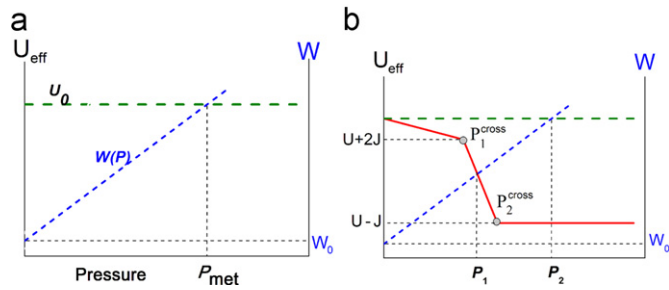


**Fig. 3.** Schematic view of the insulator–metal transition in the  $3d^5$  transition metal compounds. The pressure dependences of the d-band width  $W$  and Hubbard parameter  $U_{\text{eff}}$  are shown, and the criterion of IMT is  $W \sim U_{\text{eff}}$ . (a) In the “bandwidth control” mechanism of IMT ( $U_{\text{eff}}$  is independent of  $P$ ), crossing of the  $W(P)$  line with the  $U_0$  level indicates a possible IMT transition at high pressure  $P_{\text{met}}$ . (b) In strongly correlated electronic systems the Hubbard parameter  $U_{\text{eff}}$  depends on the  $d_4$ ,  $d_5$  and  $d_6$  spin states, and  $U_{\text{eff}}$  decreases at HS–LS crossovers which appear in  $d_4$ ,  $d_5$  and  $d_6$  configurations at different pressures (the “Hubbard energy control” mechanism). As a result, IMT occurs at pressure  $P_1$  which is much lower than  $P_2$  (in an accordance with the experimental data) [10,11].

At the same pressures, the structural phase transitions with a sharp drop of the unit cell volume were found in  $\text{FeBO}_3$  and  $\text{NdFeO}_3$  crystals [3,4]. Meanwhile, it was established that the metallization process is very complicated. In the pressure region of the HS–LS spin crossover, many crystals transformed from the dielectric to a semiconducting state. The direct insulator–metal transition (IMT) was found in  $\text{Y}_3\text{Fe}_5\text{O}_{12}$  [8] and  $\text{BiFeO}_3$  crystals [9,10].

These effects were explained by the Mott–Hubbard type transitions with the extensive suppression of strong d–d electronic correlations [10,11]. The commonly accepted mechanisms of IMT in strongly correlated d-electron systems are the band-width controlled IMT (driven by the broadening of the d-bands), and filling-controlled IMT, induced by the doping of charge carriers into the parent insulator compound.

However recently a new mechanism of IMT in Mott–Hubbard insulators have been discovered experimentally and explained theoretically [10,11]. This mechanism can be initiated by the lattice compression at high pressure and it is driven by a spin transition in  $3d^5$  ions from the high-spin (HS) state to the low-spin (LS) state (see Fig. 3). As shown in [11], the HS–LS spin-crossover suppresses the effective Hubbard parameter  $U_{\text{eff}}$  down to the value enabling the insulator–metal transition according to the Mott mechanism  $U_{\text{eff}}/W \approx 1$  ( $W$  is a half of the d-bandwidth).

This type of a Mott–Hubbard IMT was first observed experimentally in the multiferroic  $\text{BiFeO}_3$  [10], and similar mechanism must be effective for other  $3d^5$  transition-metal compounds such as  $\text{FeBO}_3$ ,  $\text{GdFe}_3(\text{BO}_3)_4$ ,  $\text{RFeO}_3$  ( $R=\text{La, Nd, Pr, Lu}$ ),  $\text{Y}_3\text{Fe}_5\text{O}_{12}$ ,  $\alpha\text{-Fe}_2\text{O}_3$ ,  $\text{Fe}_3\text{O}_4$ ,  $\text{MnO}$  where the spin crossover was found along with insulator–metal or insulator–semiconductor transitions [3]. The new IMT mechanism was call as the “Hubbard energy control” mechanism [11], to distinguish from the well known “bandwidth control” and “band-filling” mechanisms of the IMT.

### 3. Spin crossovers in $d^6$ electronic configuration and a quantum phase transition

The low spin state of transition metal ions with the  $3d^6$  electronic configuration is diamagnetic ( $S=0$ ), and the HS–LS transition [( $S=2$ ) $\rightarrow$ ( $S=0$ )] can dramatically alter the physical and chemical properties of such materials. The HS–LS spin crossover in  $3d^6$  ( $\text{Fe}^{2+}$ ) ions is a transition ( $e_g^2 \uparrow$ )( $t_{2g}^4 \uparrow$ )  $\Rightarrow$  ( $e_g^0$ )( $t_{2g}^3 \uparrow$ )( $t_{2g}^3 \downarrow$ ).

An interesting example of the HS–LS transition was recently observed in ferroperricite ( $\text{Mg,Fe}$ )O [12] which is one of the most

abundant minerals of the Earth’s lower mantle. The high pressure and low temperature investigations by TMS and SMS Mössbauer spectroscopy allowed to establish a fundamental understanding of the ground electronic and magnetic states in ( $\text{Mg}_{0.75},\text{Fe}_{0.25}$ )O [12].

It was found that the ground electronic state of  $\text{Fe}^{2+}$  at the critical pressure  $P_c$  of the spin transition and close to  $T=0$  is determined by a quantum critical point  $P_q(T=0, P_c)$  where the energy difference between the HS and LS states (an energy gap for the spin fluctuations) is zero. The deviation from  $T=0$  leads to the thermal excitations between the HS and LS states, suggesting a strong influence on the magnetic and another physical properties of the material. Our theoretical calculations indicate that the existence of the quantum critical point at zero temperature affects not only the low-temperature physical properties, but also the strong temperature/pressure-dependent properties at extreme conditions of the Earth’s lower mantle.

Based on the analyses of the Mössbauer spectra the derived hyperfine parameters of iron ions in the sample are used to construct the magnetic phase diagram and to address the quantum critical point phenomenon in ( $\text{Mg,Fe}$ )O at high pressures and low temperatures where the spin gap energy between the HS and LS states is zero. Based on the theory of the quantum spin fluctuations, we predict an appearance of new magnetic properties in ( $\text{Mg,Fe}$ )O at the high  $P$ – $T$  conditions relevant to the Earth’s lower-mantle.

Here we suggest a multielectronic model of the Mott–Hubbard insulator ( $\text{Mg}_{1-x}\text{Fe}_x$ )O. Energies of the  $d^5$ ,  $d^6$  and  $d^7$  terms are calculated in the strong electronic correlation approximation, and the energies of Hubbard fermions ( $d^5 \rightarrow d^6$  and  $d^6 \rightarrow d^7$  excitations) for HS and LS states are found. It is shown that with pressure, the HS state can either transit to metallic state or experiences the spin crossover passing a quantum critical point at  $T=0$  and  $P=P_c$ . A metallic state occurs at this point, however a semiconducting state restores with further pressure increase. At finite  $T$ , spin value fluctuations expand the pressure range of the metallic state.

At  $P > P_c$  the electronic system is the LS state when  $kT \ll \varepsilon_S$  ( $\varepsilon_S$  is the energy of spin gap, which is zero at the critical point  $P_c$ ) and it transforms (crossovers) into HS state at  $kT > \varepsilon_S$ .

### 4. Quantum phase transition in antiferromagnet with spin crossover

In the region of HS and LS states coexistence (at  $P \sim P_c$  and finite  $T$ ), the magnetic properties of a system can be described in a model of binary alloy with the Hamiltonian

$$H = \frac{1}{2} \sum_{ij\alpha\beta} p_i^\alpha p_j^\beta I_{ij}^{\alpha\beta} S_{i\alpha} S_{j\beta}, \quad (1)$$

where  $\alpha, \beta = 1, 2$  denotes the HS and LS states,  $p_i^1 = 1$  for HS and 0 for LS,  $p_i^2 = 0$  for HS and 1 for LS,  $S_{i1} = S_{\text{HS}}$ ,  $S_{i2} = S_{\text{LS}}$ , and  $I_{ij}^{\alpha\beta}$  is the exchange interaction of spin  $S_{i\alpha}$  and  $S_{j\beta}$  at sites  $i$  and  $j$ . We consider a two-sublattice (A and B) antiferromagnet. In a standard mean field theory an order parameter is a sublattice magnetization given by

$R_\alpha = \langle S_{A,\alpha}^z \rangle = \langle p^\alpha \rangle S_\alpha B_{S_\alpha}(S_\alpha y_\alpha)$ . Here  $\langle p^1 \rangle = n_{\text{HS}}$ ,  $\langle p^2 \rangle = n_{\text{LS}}$  are the fractions of HS and LS states,  $B_S(y)$  is the Brillouin function.

The effective magnetic fields are given by

$$y_1 = (g_{\text{HS}} \mu_B H + n_{\text{HS}} I^{11}(0) R_1 + n_{\text{LS}} I^{12}(0) R_2) / k_B T,$$

$$y_2 = (g_{\text{LS}} \mu_B H + n_{\text{HS}} I^{21}(0) R_1 + n_{\text{LS}} I^{22}(0) R_2) / k_B T \quad (2)$$

The value  $I^{\alpha\beta}(0)$  is the Fourier transform of the exchange interaction for wavenumber  $q=0$ ,  $\mu_B$  is the Bohr magneton,  $H$  is the external magnetic field, and  $k_B$  is the Boltzman constant. Close

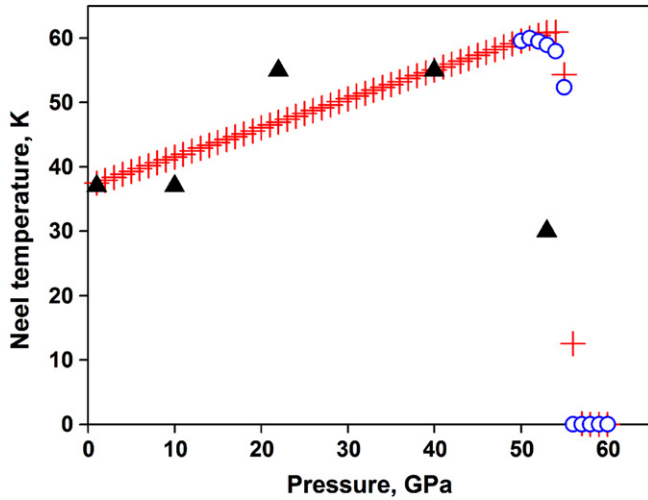


**Fig. 4.** Pressure dependence of the Neel temperature in the antiferromagnet ( $\text{Mg}_{0.75}\text{Fe}_{0.25}\text{O}$ ) with spin-crossover at  $P_c=55$  GPa. Non-self consistent (red crosses) and self consistent (empty blue circles) calculated data are compared with experimental data (black triangles) [12]. (For interpretation of the references to color in this figure legend, the reader is referred to the web version of this article.)

to the Neel temperature  $T_N$ , linearization of the Brillouin function results in a system of equations for  $R_c(T, H)$ . At  $H=0$  and for  $S_{LS}=0$ , f. e. in  $\text{Fe}^{2+}$ , the Neel temperature is equal to

$$T_N = T_{N0} n_{\text{HS}}^2(p, T_N). \quad (3)$$

For a binary alloy with fixed concentration of the magnetic HS and non-magnetic LS fractions, the Eq. (3) gives the  $T_N$  value in a case of diamagnetic substitution. Meanwhile in our case,  $n_{\text{HS}}$  and  $n_{\text{LS}}$  are pressure and temperature dependent. At fixed volume, they are equal to

$$n_{\text{HS}} = \left[ 1 + \frac{g_{\text{LS}}}{g_{\text{HS}}} \exp\left(\frac{E_{\text{HS}} - E_{\text{LS}}}{kT}\right) \right]^{-1} \rightarrow n_{\text{LS}} = 1 - n_{\text{HS}}, \quad (4)$$

Thus, the Eq. (3) is a self-consistent equation for the  $T_N$  in the vicinity of  $P_c$ . Far from  $P_c$ , one should include the pressure dependence of the  $T_{N0} = I^{11}(0)S_1(S_1 + 1)/3k_B$ . The nearest neighbor exchange interaction is  $J = 2t^2/U$ , where  $t$  is the d-d hopping and  $U$  is the effective Hubbard parameter. We assume  $U$  to be pressure independent and  $t(P) = t_0(1 + \alpha_t P)$  [13]. Then

$$T_{N0}(P) = T_{N0}(0) \left( 1 + \frac{2\alpha_t P}{t} \right).$$

From the experimental data for  $\text{Mg}_{1-x}\text{Fe}_x\text{O}$ ,  $T_N=37$  K at  $P=0$  and  $T_N=55$  K at  $P=55$  GPa [12]. Thus,  $2\alpha_t t_0 = 0.0122$  1/GPa is very close to the value  $2\alpha_t t_0 = 0.0121$  1/GPa found for  $\text{FeBO}_3$  from the high pressure experiments [14]. The spin gap  $\varepsilon_S = E_{\text{HS}} - E_{\text{LS}}$  is also linear dependent on  $P$  due to the pressure dependence of the crystal field  $10Dq(P) = 10Dq(0) + \alpha_\Delta P$ . The quantum critical point  $P_c$  is determined by a zero spin gap  $\varepsilon_S = \alpha_\Delta(P - P_c)$ . Finally, the pressure dependence of Neel temperature is given by a solution of

the equation

$$T_N = T_{N0}(0) \left( 1 + \frac{2\alpha_t P}{t_0} \right) / \left[ 1 + \frac{g_{\text{LS}}}{g_{\text{HS}}} \exp\left(\frac{\alpha_\Delta(P - P_c)}{kT_N}\right) \right]^2 \quad (5)$$

The degeneracy factors are  $g_{\text{LS}}=1$  for the LS- $\text{Fe}^{2+}$  state and  $g_{\text{HS}}=(2S+1)(2L+1)=15$  for the HS- $\text{Fe}^{2+}$  state. The baric dependence of a spin gap is  $\alpha_\Delta=7.8$  meV/GPa [12]. Numerical solution of this equation results in a first order quantum phase transition shown in the Fig. 4 by empty circles.

The  $T_N$  increases at small  $P$ , reaches a maximum and does not go continuously to zero at  $P \rightarrow P_c$ . Instead, it has the critical value  $T_N/T_{N0}(0) = g_{\text{HS}}^2 / (g_{\text{HS}} + g_{\text{LS}})^2 \approx 0.879$  at  $P \rightarrow P_c$ . The non-self consistent dependence  $T_N(P)$  given by Eq. (3) with the HS fraction (4) would result in the continuous line shown by crosses in Fig. 4. Black triangles correspond to the measured value of  $T_N(P)$  for  $\text{Mg}_{0.75}\text{Fe}_{0.25}\text{O}$  [12].

Previously, the order parameter at spin crossover quantum phase transition was shown to be the Berry-like geometrical phase that changes discontinuously by a first-order transition [15,16]. Thus, our microscopic consideration in this paper confirms a phenomenological treatments [15,16]. Usually, a long magnetic order at  $T=T_N$  is destroyed by classical spin fluctuations. Since the spin-crossover quantum fluctuations of the spin value between HS and LS states do not require any energy, the antiferromagnetism is destroyed in the quantum critical point by the first order transition.

## Acknowledgments

We acknowledge the help and discussions with Drs. A.G. Gavriiliuk, V.V. Struzhkin and J.F. Lin. Supports by RFBR (Grants # 09-02-00171, 10-02-00251, # 11-02-00636, # 11-02-00291, # 11-02-12089) and by the RAS Program "Strongly correlated electronic systems" are acknowledged.

## References

- [1] N.F. Mott, Metal-Insulator Transitions, Taylor and Francis, London, 1990.
- [2] R.E. Cohen, I.I. Mazin, D.G. Isaak, Science 275 (1997) 654.
- [3] I.S. Lyubutin, A.G. Gavriiliuk, V.V. Struzhkin, in: M.R. Manaa, A.F. Goncharov, R.J. Hemley, R. Bini (Eds.), Materials Research at High Pressure, 987, Warrendale, Pennsylvania, 2007, pp. 167–178, total 199 pages.
- [4] I.S. Lyubutin, A.G. Gavriiliuk, Physics Uspekhi 52 (2009) 989–1017.
- [5] V.A. Sarkissyan, I.A. Trojan, I.S. Lyubutin, A.G. Gavriiliuk, A.F. Kashuba, JETP Letters 76 (2002) 664–669.
- [6] A.G. Gavriiliuk, V.V. Struzhkin, I.S. Lyubutin, M.Y. Hu, H.K. Mao, JETP Letters 82 (2005) 224–227.
- [7] I.S. Lyubutin, A.G. Gavriiliuk, V.V. Struzhkin, JETP Letters 88 (2008) 524–530.
- [8] A.G. Gavriiliuk, V.V. Struzhkin, I.S. Lyubutin, I.A. Trojan, JETP Letters 82 (2005) 603–608.
- [9] A.G. Gavriiliuk, I.S. Lyubutin, V.V. Struzhkin, JETP Letters 86 (2007) 532–536.
- [10] A.G. Gavriiliuk, V.V. Struzhkin, I.S. Lyubutin, S.G. Ovchinnikov, M.Y. Hu, P. Chow, Physical Review B 77 (2008) 155112–1–6.
- [11] I.S. Lyubutin, S.G. Ovchinnikov, A.G. Gavriiliuk, V.V. Struzhkin, Physical Review B 79 (2009) 085125–1–085125–7.
- [12] I.S. Lyubutin, V.V. Struzhkin, A.A. Mironovich, A.G. Gavriiliuk, P.G. Naumov, J.F. Lin, S.G. Ovchinnikov, S. Sinogeikin, P. Chow, and Y. Xiao, Nature Communications (in press).
- [13] S.G. Ovchinnikov, Journal of Physics: Condensed Matter 17 (2005) S743.
- [14] A.G. Gavriiliuk, I.A. Trojan, I.S. Lyubutin, V.A. Sarkissian, S.G. Ovchinnikov, Journal of Experimental and Theoretical Physics 100 (2004) 688.
- [15] A.I. Nesterov, S.G. Ovchinnikov, Physical Review E 78 (2008) 015202.
- [16] A.I. Nesterov, S.G. Ovchinnikov, JETP Letters 90 (2009) 530.